Preparatin and investigation of $Ni_{1-x}Zn_xFe_2O_4$ nanoparticles: the effect of x parameter on the magnetic properties

G. R. AMIRI*, M. H. YOUSEFI[a], S. FATAHIAN
Falavarjan Branch, Islamic Azad University, Isfahan, Iran
[a]*Department of sciences, Nano-center, Malek-ashtar University of Technology, Isfahan, Iran*

$Ni_{1-x}Zn_xFe_2O_4$ nanoparticles (a few nm in diameter) were produced by low-temperature solid-state reaction (LTSSR) method. Magnetic and structural properties of the products were investigated by scanning tunneling microscopy (STM), X-ray diffraction (XRD), alternating gradient-force magnetometery (AGFM) and transmission electron microscopy (TEM). The Curie temperature was also determined for several samples. Energy dispersive X-ray (EDX), X ray fluorescence (XRF) and atomic absorption spectroscopy (AAS) analysis were taken from some samples in order to recheck the elemental results. The effect of x parameter on saturation magnetization was studied. It was found that the maximum saturation magnetization occurred at x=0.5 ($Ni_{0.5}Zn_{0.5}Fe_2O_4$).

(Received April 21, 2012; accepted June 6, 2012)

Keywords: Ferrite, Superparamagnetic nanoparticles

1. Introduction

Ni-Zn ferrites were synthesized about 60 years ago for the first time. They have been commercially used as high-frequency ferrites for radio frequency coils and transformer cores. The spinel ferrites crystallize in an FCC lattice with eight formula units in the cubic cell. Two fundamental limits can be distinguished, namely normal and inverse spinels. The composition of ferrospinels can be described by the general formula $M^{+2}[Fe^{+3}Fe^{+3}]O_4$ [1]. However, the unusual distribution of cations among the oxygen coordinated tetrahedral (T) and octahedral (O) sites is an important factor for explanation of the catalytic effectiveness [1]. On the other hand, it seems that small rare-earth additions can modify the structure and magnetic properties of Ni-Zn ferrites with direct influence on their resistivity and permeability. Thus, there is an increasing interest for production of new magnetic nanoparticles and understanding their unusual properties compared to those of bulk samples, due to their wide range of applications [2-6] .

In this study, $Ni_{1-x}Zn_xFe_2O_4$ nanoparticles were prepared by using LTSSR (Low Temperature Solid-State Reaction) method, previously reported for the preparation of simple oxides, such as NiO, MnO and ZnO [7-9]. This procedure has been chosen in order to avoid ball milling to get superparamagnetic $Ni_{1-x}Zn_xFe_2O_4$ nanoparticles.

2. Experimental

The chemical reagents are high purity ferric chloride ($FeCl_3.6H_2O$), nickel chloride ($NiCl_2.6H_2O$), zinc chloride ($ZnCl_2$) and sodium hydroxide (NaOH), from Merck Company. The powders were mixed in their stoichiometric ratios. For instance, in order to synthesize $Ni_{0.5}Zn_{0.5}Fe_2O_4$ nanoparticles, the stoichiometric ratio was calculated 0.5:0.5:2:8. Thus 1.188gr of $NiCl_2.6H_2O$, 0.681gr of $ZnCl_2$, 5.404gr of $FeCl_3.6H_2O$ and 3.2gr of NaOH were mixed together. Then the mixture was grinded uniformly in an agate mortar for about 30 min. After this stage, the nanoparticles were washed with water and acetone several times to remove remaining impurities [4].

In order to obtain nanoparticles with general formula $Ni_{1-x}Zn_xFe_2O_4$ the following reaction was used, with *x* changing from 0.1 to 0.9.

$$xZnCl_2 + (1-x)NiCl_2 + 2FeCl_3 + 8NaOH \rightarrow Ni_{1-x}Zn_xFe_2O_4 + 4H_2O + 8NaCl$$

XRD (X-Ray Diffraction, Bruker D8 ADVANCE λ=0.154nm Cu Kα radiation), STM (Scanning Tunneling Microscope, NATSICO Iran) and TEM (Transmission Electron Microscopy) were used to investigate the particles size distribution.

The structural coherence length can be calculated by the Scherrer equation:

$$D = \frac{0.9\lambda}{\beta \cos\theta}$$

Where D is the crystalline size in nm, λ the Cu-Kα wavelength (0.154nm), β is the half-width of the peak in radians (instrumental line width subtracted) and θ is the corresponding diffraction angle [7].

Magnetic properties of nanoparticles were assessed by AGFM (Alternating Gradient-Force Magnetometer, Meghnatis Daghigh Kavir Co, Iran) up to 9 kOe external magnetic field at room temperature. The Curie temperature

was determined by Faraday balance equipment in the presence of 0.12 Tesla external magnetic field.

For further assurance, EDX (Energy Dispersive X-ray), XRF (X Ray Fluorescence) and AAS (Atomic Absorption Spectroscopy) analysis were taken on some samples in order to recheck the compositional results.

3. Results and discussion

3.1. Particle size determination

XRD patterns of $Ni_{1-x}Zn_xFe_2O_4$ (x=0.1, 0.3, 0.5, 0.7 and 0.9) nanoparticles were shown in Fig. 1. As can be seen, all of samples have single phase and also have the ferrite spinel structure. The mean size of the particles was determined by Debye-Scherer formula. It was found less than 4nm for all samples (Details are shown in Table 1).

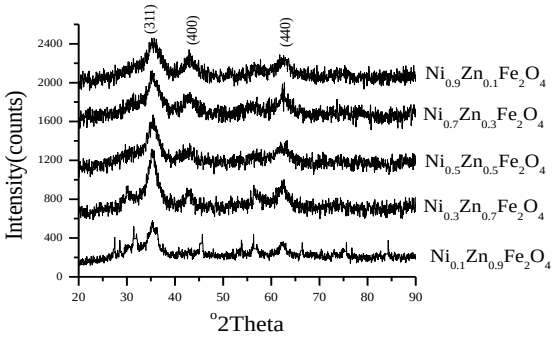

Fig. 1. XRD patterns of the $Ni_{1-x}Zn_xFe_2O_4$ samples (x=0.1, 0.3, 0.5, 0.7 and 0.9).

Fig. 2 illustrates the TEM photograph of the $Ni_{0.7}Zn_{0.3}Fe_2O_4$ sample. It can be seen that, there is a uniform size distribution approximately in whole of the photograph. It means that the synthesis manner has been suitable. The size of the particles was determined around 6 nm from TEM photograph.

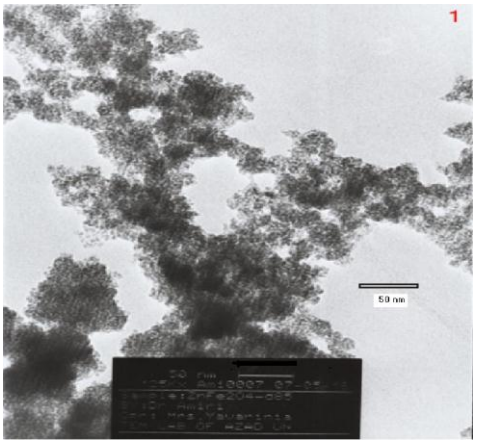

Fig. 2. Transmission Electron Micrograph of $Ni_{0.7}Zn_{0.3}Fe_2O_4$.

Fig. 3 demonstrates the STM photograph of the $Ni_{0.5}Zn_{0.5}Fe_2O_4$ sample. The size was determined around 7 nm from STM photograph. By considering that the TEM and STM photographs are from 2 different nanoparticles which have the same structure, it is concluded that the results of both photographs have good agreement with each other.

On the other hand, the difference between the particles estimated size from the STM and TEM photographs in comparison with the XRD pattern is related to their accuracy.

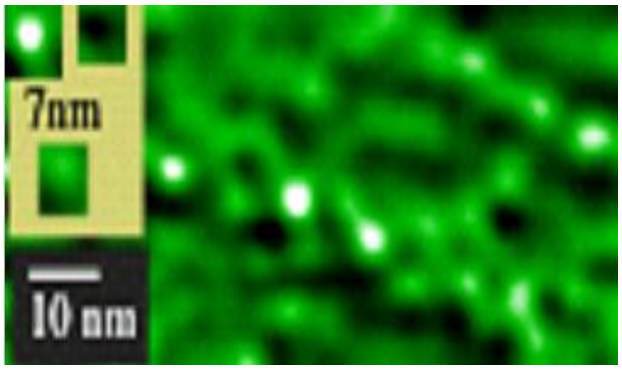

Fig. 3. Scaning Tunneling Microscopy of $Ni_{0.5}Zn_{0.5}Fe_2O_4$.

3.2. Assessment of magnetic properties by AGFM

The results of the AGFM measurements for $Ni_{1-x}Zn_xFe_2O_4$ (x=0, 0.1, 0.3, 0.5, 0.7 and 0.9) nanoparticles are given in Fig. 4. The variations of the relative magnetization in these figures and also the lack of remanence magnetization, demonstrate the super paramagnetic behavior of the samples. As can be seen, all samples cannot reach to the saturation state in the presence of a relatively strong magnetic field of even 9 kOe. The saturation magnetization (Ms) can be determined by extrapolation of magnetization curve on the basis of $\frac{1}{H}$ when $\frac{1}{H} \to 0$.

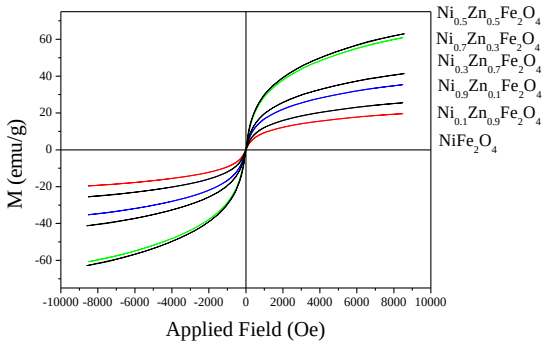

Fig. 4. AGFM plot of magnetization versus applied field up to 9kOe for $Ni_{1-x}Zn_xFe_2O_4$ samples (x=0, 0.1, 0.3, 0.5, 0.7 and 0.9).

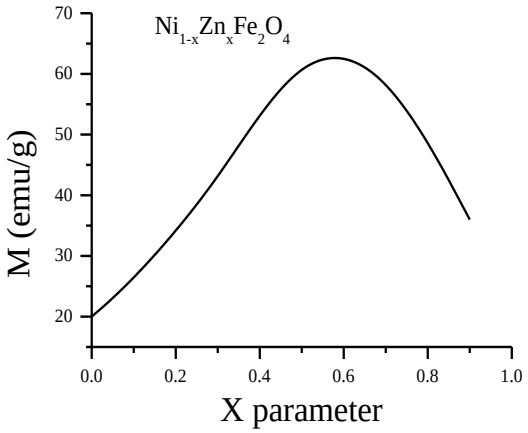

Fig. 5. Dependency of $Ni_{1-x}Zn_xFe_2O_4$ magnetization to X parameter (x=0, 0.1, 0.3, 0.5, 0.7 and 0.9) at 9kOe magnetic field.

Fig. 5 shows the dependency of $Ni_{1-x}Zn_xFe_2O_4$ magnetization to x parameter observed by AGFM, for (x=0, 0.1, 0.3, 0.5, 0.7 and 0.9). The magnetizations of the nanoparticles were obtained in the 9 kOe external magnetic field. It can be seen that, the magnetization of the sample has the maximum value at x=0.5. Thus, the results confirm with that of bulk ones.

The magnetization dependency to the temperature for some $Ni_{1-x}Zn_xFe_2O_4$ samples (x=0, 0.1, 0.5 and 0.7) are shown in Fig. 6. The Curie temperatures (Tc) were measured by the Faraday balance technique at the 0.12 Tesla external magnetic field. The results are listed in Table 1. The Curie temperature is smaller than that of bulk ones for all samples. The Curie temperature is also strongly depended on the variation of the x-parameters. For instance, it was determined 404 ^{0}C and 274 ^{0}C for x=0 and x=0.7 respectievly.

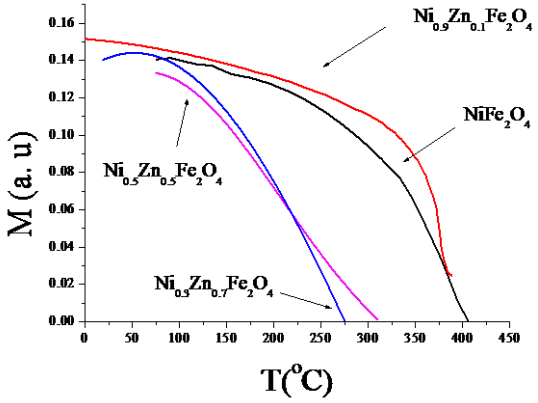

Fig. 6. Dependency of magnetization to temperature for $Ni_{1-x}Zn_xFe_2O_4$ samples (x=0, 0.1, 0.5 and 0.7). B=0.12 T.

Table 1. The physical properties of the $Ni_{1-x}Zn_xFe_2O_4$ samples.

specimen	M (emu/g) 9 kOe	T_C (^{0}C)	D(nm) XRD	D(nm) STM	D(nm) TEM
$NiFe_2O_4$	20	404	--	--	--
$Ni_{0.9}Zn_{0.1}Fe_2O_4$	36	382	2.5	--	--
$Ni_{0.7}Zn_{0.3}Fe_2O_4$	62	--	3	--	6
$Ni_{0.5}Zn_{0.5}Fe_2O_4$	64	309	3.8	7	--
$Ni_{0.3}Zn_{0.7}Fe_2O_4$	42	274	4	---	--
$Ni_{0.1}Zn_{0.9}Fe_2O_4$	26	--	3	---	--

EDX, AAS and XRF results from the stoichiometric ratios of some sample are shown in Table 2, 3 and 4. The results of EDX and AAS analysis for x=0.5 are listed in Table 2 and Table 3, respectively. Also the results of XRF for x=0.3 are listed in Table 4. The primary atomic stoichiometric percentage is the ratio of each element or compound we used in the synthesis process. It can be seen that the primary atomic stoichiometric ratios and percentages are approximately around the atomic percentages which are obtained from the EDX, AAS and XRF results. Small differences between the primary stoichiometric ratios and the atomic percentages which are obtained from the EDX, AAS and XRF results can help us to select an optimum primary stoichiometric ratio.

Table 2. EDX results for $Ni_{0.5}Zn_{0.5}Fe_2O_4$ samples.

Ions	Primary Atomic Stoichiometric Percentage	Final Atomic Percentage From EDX
Fe	71	67.72
Ni	18.9	22
Zn	9.6	10.27

Table 3. AAS results for $Ni_{0.5}Zn_{0.5}Fe_2O_4$ samples.

Ions	Primary Atomic Stochiometric Percentage	Final Atomic Percentage From AAS
Fe	71	67
Ni	18.9	20
Zn	9.6	10.7

Table 4. XRF results for $Ni_{0.7}Zn_{0.3}Fe_2O_4$ samples.

Ions	Primary Atomic Stochiometric Ratio	Stochiometric Ratio From XRF
Ni/Fe	0.35	0.35
Zn/Fe	0.157	0.15

4. Conclusions

In this study, LTSSR method was used to produce the $Ni_{1-x}Zn_xFe_2O_4$ nanostructure crystals with different values for x variable. The nanoparticle sizes were determined a few nanometer (less than 7 nm) for different x values. It is concluded from Fig. 4, 5 and 6 that the physical and magnetic properties of the samples were strongly depended on the x parameter value. From the results of Fig. 6, it is also concluded that the Curie temperature is reduced by increasing the presence of zinc ion.

All samples cannot reach to the saturation magnetization state at the presence of a relatively strong magnetic field of even 9 kOe. The x parameter was changed from 0.1 to 0.9 by steps of 0.2 and the maximum magnetization was occurred in $Ni_{0.5}Zn_{0.5}Fe_2O_4$ (x=0.5).

Small differences between the primary atomic stoichiometric ratios and the atomic percentages which are obtained from the EDX, AAS and XRF results can help us to select an optimum primary stoichiometric ratio in the future studies. It is suggested to investigate the effect of x parameter on the physical and magnetic properties of other nanoparticles for other metals instead of zinc.

References

[1] B. D. Cullity, Introduction to Magnetic Materials, Addison-Wesley, New York (1972).
[2] Gh. R. Amiri, M. H. Yousefi, S. Fatahian, J. Optoelectron. Adv. Mater.-Rapid Commun. **6**(1-2), 158 (2012).
[3] R. H. Kodama, A. E. Berkowitz, Phys. Rev. B, **59**, 6321 (1999).
[4] Gh. R. Amiri, M. H. Yousefi, M. R. Aboulhassani, M. H. Keshavarz, S, Manouchehri, S. Fatahian, J. Magn. Magn. Mater, **323**,730-734 (2011).
[5] S. Fatahian, D. Shahbazi, M. Pouladian, M. H. Yousefi, Gh. R. Amiri, Z. Shahi, H. Jahanbakhsh, Digest Journal of Nanomaterials and Biostructures, **6**(3), 1161 (2011).
[6] M. M. Hessien, J. Magn. Magn. Mater, **320**, 2800 (2004).
[7] Gh. R. Amiri, M. H. Yousefi, M. R. Aboulhassani, M. H. Keshavarz, D. Shahbazi, S. Fatahian, M. Alahi, Digest Journal of Nanomaterials and Biostructures, **5**(3), 1025 (2010).
[8] Gh. R. Amiri, S. Fatahian, A. R. Jelvani, R. Mousarezaei, M. Habibi, J. Optoelectron. Adv. Mater.-Rapid Commun. **5**(11), 1178 (2011).
[9] A. R. Jelvani, Gh. R. Amiri, S. Fatahian, S. Manouchehri, M. Habibi, R. Mousarezaei, J. Optoelectron. Adv. Mater.-Rapid Commun. **5**(11), 1216 (2011).

*Corresponding author: amiri@iaufala.ac.ir